Bone 127 (2019) 82–90

Contents lists available at ScienceDirect

Bone

journal homepage: www.elsevier.com/locate/bone

Full Length Article

Quantitative ultrasound (QUS) axial transmission method reflects anisotropy in micro-arrangement of apatite crystallites in human long bones: A study with 3-MHz-frequency ultrasound

Takuya Ishimoto[a,1], Ryoichi Suetoshi[b,1], Dorian Cretin[b], Koji Hagihara[c], Jun Hashimoto[d], Akio Kobayashi[e], Takayoshi Nakano[a,*]

[a] Division of Materials and Manufacturing Science, Graduate School of Engineering, Osaka University, 2-1, Yamada-Oka, Suita, Osaka 565-0871, Japan
[b] Research and Innovation Center, Furuno Electric Co., Ltd., 9-52, Ashihara-cho, Nishinomiya, Hyogo 662-8580, Japan
[c] Department of Adaptive Machine Systems, Graduate School of Engineering, Osaka University, 2-1, Yamada-Oka, Suita, Osaka 565-0871, Japan
[d] Department of Rheumatology, National Hospital Organization, Osaka-Minami Medical Center, 2-1 Kidohigashi, Kawachinagano, Osaka 586-8521, Japan
[e] Department of Orthopaedic Surgery, Shiraniwa Hospital Joint Arthroplasty Center, 6-10-1 Shiraniwadai Ikoma, Nara 630-0136, Japan

ARTICLE INFO

Keywords:
Speed of sound (SOS)
Leaky surface wave
Anisotropy
Apatite orientation
Bone quality

ABSTRACT

Anisotropic arrangement of apatite crystallites, i.e., preferential orientation of the apatite *c*-axis, is known to be an important bone quality parameter that governs the mechanical properties. However, noninvasive evaluation of apatite orientation has not been achieved to date. The present paper reports the potential of quantitative ultrasound (QUS) for noninvasive evaluation of the degree of apatite orientation in human bone for the first time. A novel QUS instrument for implementation of the axial transmission (AT) method is developed, so as to achieve precise measurement of the speed of sound (SOS) in the cortex (cSOS) of human long bone. The advantages of our QUS instrument are the following: (i) it is equipped with a cortical bone surface-morphology detection system to correct the ultrasound transmission distance, which should be necessary for AT measurement of long bone covered by soft tissue of non-uniform thickness; and (ii) ultrasound with a relatively high frequency of 3 MHz is employed, enabling thickness-independent cSOS measurement even for the thin cortex by preventing guide wave generation. The reliability of the proposed AT measurement system is confirmed through comparison with the well-established direct transmission (DT) method. The cSOS in human long bone is found to exhibit considerable direction-dependent anisotropy; the axial cSOS (3870 ± 66 m/s) is the highest, followed by the tangential (3411 ± 94 m/s) and radial (3320 ± 85 m/s) cSOSs. The degree of apatite orientation exhibits the same order, despite the unchanged bone mineral density. Multiple regression analysis reveals that the cSOS of human long bone strongly reflects the apatite orientation. The cSOS determined by the AT method is positively correlated with that determined by the DT method and sensitively reflects the apatite orientation variation, indicating the validity of the AT instrument developed in this study. Our instrument will be beneficial for noninvasive evaluation of the material integrity of the human long-bone cortex, as determined by apatite *c*-axis orientation along the axial direction.

1. Introduction

Quantitative ultrasound (QUS) can be employed for noninvasive bone evaluation. Unlike X-rays, ultrasound does not involve radiation exposure; thus, it can be safely applied to patients of all ages. A device for measuring calcaneus bone density with ultrasound has already been used for osteoporosis screening [1]. Like the vertebral body, the calcaneus is rich in cancellous bone, which is generally susceptible to metabolic diseases [2]; therefore, ultrasound is suitable for screening of metabolic diseases. In recent years, increasing attention has been directed towards the fracture risk of cortical bone, e.g., fractures in the proximal femur and femoral neck; thus, the importance of cortical bone evaluation has been emphasized [3,4].

Attempts have been made to use ultrasonic waves for cortical bone measurement. As ultrasound utilizes elastic waves and the ultrasonic velocity reflects the elastic properties of the propagating material, this

* Corresponding author.
E-mail address: nakano@mat.eng.osaka-u.ac.jp (T. Nakano).
[1] These authors contributed equally to this work.

https://doi.org/10.1016/j.bone.2019.05.034
Received 24 April 2019; Received in revised form 20 May 2019; Accepted 26 May 2019
Available online 03 June 2019

technique is expected to be useful for evaluating the material properties of cortical bone. For ultrasonic evaluation of long cortical bones, the axial transmission (AT) technique is used, in which an ultrasonic transmitter/receiver pair is placed parallel to the bone longitudinal axis on one side. Ultrasound with a frequency of < 1.5 MHz is mainly used in the AT method [5–10], which is equivalent to a wavelength of approximately 2.7 mm (at 1.5 MHz), assuming that the ultrasonic velocity in the axial direction is 4000 m/s. The sound-wave propagation velocity is influenced by a structure with a dimension similar to the wavelength [11]. As cortical bone has a thickness of several millimeters, which is comparable to the wavelength, it is necessary to note the effect of the cortical thickness on the speed of sound (SOS). If the cortex thickness is not considered in cases where it is low relative to the wavelength, the apparent cortical SOS (cSOS) will decrease because of the generation of guide waves [12], yielding incorrect estimation of the material properties. In other words, the thickness effect interferes with the evaluation of the intrinsic material properties. Independent estimation of cSOS and cortical thickness from guided waves has recently been reported [13,14]. In such cases, the cortex is assumed to be a two-dimensional transverse isotropic free plate. However, this structure is not necessarily appropriate for simulating the actual cortex shape, particularly for the bones of the elderly. Thus, there is some concern regarding the robustness of the cSOS measurement.

The materials properties of the cortical bones are largely affected by their micro-organization. In particular, it is understood that the crystallographic texture and orientation of the bone matrix elements (mainly the type-I collagen and apatite) strongly regulate the functions of the bone materials. Indeed, despite their similar bone mineral density (BMD), the direction, dimension, and degree of preferential orientation of collagen and apatite vary largely depending on the anatomical bone type and site [15]. AT measurements have been reported to reflect details of the macroscopic bone structure, i.e., the cortical thickness and porosity [14] and BMD [16]. However, it is important to clarify whether the AT method reflects the collagen/apatite micro-arrangement independently of the thickness effect. Recently, the present authors emphasized that the preferential orientation of the apatite *c*-axis contributes significantly to the mechanical function of bone [17,18]. This behavior arises because apatite has a hexagonal-based lattice showing anisotropy in the intrinsic mechanical properties such as the Young's modulus [19]. Thus, the anisotropic arrangement of the apatite is an important factor governing the mechanical properties of bone. However, the biggest hindrance to consideration of preferential apatite orientation for clinical use is the lack of a noninvasive evaluation method.

In this study, we develop an AT system with a relatively high 3-MHz-frequency ultrasound probe for human long bones. This frequency is employed to eliminate the guided wave generation and thickness effect, as 3-MHz frequency corresponds to a wavelength of approximately 1.3 mm. Further, the cortical thickness range in which the material properties can be accurately evaluated expands under the usage of higher-frequency ultrasound. Thus, 3-MHz frequency is expected to be effective for evaluation of osteoporotic bone with a thinned cortex. Bone thickness can be easily evaluated through conventional X-ray radiography and computed tomography (CT); hence, we aim to develop a specialized device for investigation of the material properties of cortical bone, which are almost undetectable using X-ray radiography and CT.

As the signal attenuation rate is high at higher frequencies such as 3 MHz, and because it is difficult to detect sonic waves with small amplitudes at distant receivers, we utilize a probe with linearly arrayed multiple receivers and a bone shape detection/correction system to achieve measurement with a good signal-to-noise ratio and accuracy. To validate our system, the obtained results are first compared with those determined via the well-defined direct transmission (DT) method for which the ultrasonic transmitter and receiver are placed on opposite sides of the measuring object. Then, the origin of the anisotropy in the cSOS in human long bone is examined, focusing on the variations in the preferential apatite orientation as an anisotropic feature of the bone material quality and the volumetric BMD (vBMD).

2. Materials and methods

In this study, the cSOS of the human long-bone cortex was measured using the following setup. The aim was to demonstrate the validity of our QUS-AT system and to investigate whether the AT method can detect preferential apatite orientation in the cortex, which contributes to the mechanical functions of the bone.

2.1. Study setup

The study was divided into two stages, labeled “Study_1” and “Study_2,” respectively. In Study_1, the correlation between the tri-directional (axial, tangential, and radial) anisotropy in the cSOS and that in the bone microstructure or vBMD (corresponding to the cortex material characteristics) was first investigated via the well-defined DT method, so as to determine the contributory factors to cSOS. Rectangularly cut bone specimens were measured. On the basis of the results, the appropriateness of the QUS measurement in the “axial direction” in which the most of AT measurements have conducted, was discussed. In Study_2, the AT method was implemented using the developed instrument described below. To validate our system, the DT method was implemented subsequent to the AT measurement by preparing rectangular bone specimens from the specimens used for AT measurement. Because of donor restrictions, both studies were performed on separate cadaver groups.

2.2. Ultrasound frequency selection

We selected a relatively high 3 MHz ultrasound for the AT method. In the AT method, high-frequency ultrasound is advantageous for bone thickness-independent cSOS measurement. In contrast, as the frequency increases, scattering attenuation within the specimen increases and the signal level weakens [20]. In other words, the suppression of the scattering attenuation and the reduction of the sample thickness capable of thickness-independent measurement are in a trade-off relationship with respect to frequency. Therefore, the ultrasound frequency must be carefully selected.

We estimated the appropriate frequency based on typical human cortical bone thickness, which is reported to range from 1 to 7 mm [21]. According to Bossy et al. [21], when using 3 MHz ultrasound, the lower limit of bone thickness that enables bone thickness-independent cSOS measurement was estimated to be 0.7 mm, which is smaller than the lower limit of the typical range (1 mm), when assuming that the cSOS is approximately 4000 m/s and the bone material is anisotropic. Therefore, we selected a 3 MHz frequency. Refer to the Discussion section for more details. For validating our QUS-AT method, 3 MHz ultrasound was also used in all DT measurements.

2.3. Instrument for ultrasonic measurements

2.3.1. DT method of Study_1

The appearance of the apparatus used in the DT method and the corresponding schematic are shown in Fig. 1(a). Transmitter and receiver transducers with a center frequency of 3 MHz (Nihon Dempa Kogyo, Tokyo, Japan) were used, which were placed at opposing positions to sandwich a blocked cortical bone specimen via a 2-mm acrylic standoff. The distance was measured by a displacement encoder (LGF-0525L, Mitsutoyo, Kawasaki, Japan) and a pulse counter (PXI-6602, National Instruments, Austin, USA). Prior to specimen measurement, the standoff was directly contacted and a reference waveform was acquired. Then, the cortical bone block was sandwiched between the standoffs for acquisition of a transmission waveform. The transmitted signal was generated by a 14-bit digital-to-analog converter (PXI-5412,

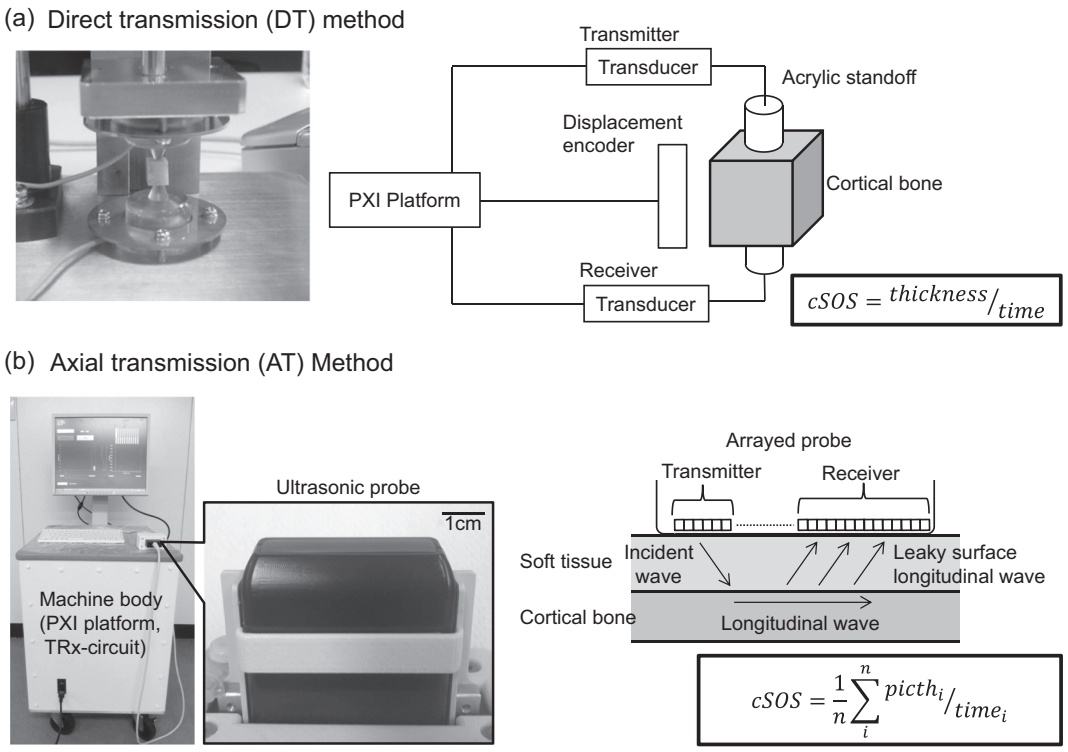

Fig. 1. Photographs and schematic illustrations of instruments and setups for QUS measurements for (a) DT and (b) AT methods.

National Instruments) at a clock frequency of 100 MHz. The receiving signal was amplified (HFA 4101, NF Corporation, Yokohama, Japan). The cSOS was calculated from the time difference and propagation distance (specimen thickness) of the first arriving signal (FAS), as shown in Fig. 1(a). The controlling, sampling, and analysis software was developed using LabView (National Instruments).

2.3.2. Configuration and features of developed AT method instrument for Study_2

To measure the cSOS propagating in the cortical bone along the long axis (the principal stress direction) from outside the skin, the AT method was adopted, as shown in Fig. 1(b). An array probe with 3-MHz center frequency was used (Nihon Dempa Kogyo). Inside the probe, 32 transmitter/receiver elements are arranged at 1 mm intervals. The signals were generated by a digital waveform generator (PXI-6542, National Instruments) and ultrasonic waves were obliquely irradiated from the transmitter to the cortical bone. The obliquely irradiated sound wave generated a leaky surface skimming compressional wave (LSSCW) on the soft tissue side, whereas a longitudinal wave propagated in the cortical bone along its long axis. The LSSCW was detected by receivers with known distances and the cSOS was derived from the distance and time for longitudinal wave propagation within the cortex [22]. The receiving signals were amplified and sampled by a 12-bit analog-to-digital-converter (PXI-5105, National Instruments) at a clock frequency of 60 MHz. The controlling, sampling, and analysis software was developed using LabView (National Instruments).

In the AT method, cSOS can be calculated correctly when the cortical bone surface and the array wave receiver are arranged in parallel. However, as regards actual measurement of human subjects *in vivo*, the soft tissue surface and the cortical bone surface are not parallel to each other and the bone surface is curved; therefore, errors are generated in the measured cSOS. For accurate cSOS calculation, it is necessary to comprehend the positional relationship between the array probe and the cortical bone surface, which can then be utilized to correct the propagation path. Thus, the instrument developed in this study employs a two-step transmission/reception system including a cortical bone surface monitoring phase and an AT measurement phase (Fig. 2(a)), which is enabled by a probe with linearly arrayed multiple receivers.

In the cortical bone surface monitoring phase, ultrasonic waves are emitted simultaneously from all the channels to generate a plane wave. Reflected echoes are received on each channel; the angle of the bone surface is calculated from the time difference in the reception of reflected echoes between adjacent channels (U.S. patent 8,372,007).

In the AT measurement phase (Fig. 2(b)), an ultrasonic wave obliquely irradiates from the transmitters located at one end, and the signals are received the other receivers. The SOS of subcutaneous soft tissue was assumed to be equal to that of water, 1500 m/s. When an ultrasonic wave obliquely irradiates the cortical bone, the array receiver receives not only the necessary LSSCW signal, but also other interfering echoes, such as direct and reflected waves from the front and back surfaces of the cortical bone. Of these, the wave reflected from the back surface of the cortex generates an error in the calculated cSOS, as its arrival time is close to that of the LSSCW. In particular, when the cortical bone is thin, the two waves are superimposed, yielding significant reduction in the cSOS. Use of a 32-fold array receiver allows the unnecessary echoes to be neglected as the received signals are processed with the optimum number of plural elements. Moreover, even if the cortical bone surface is curved, the cSOS can be calculated accurately as the bone shape is measured.

2.4. Accuracy verification of developed instrument

In this study, to estimate the SOS measurement accuracy, an acrylic plate with sufficient thickness (20 mm) compared with the wavelength (approximately 0.9 mm) was repeatedly measured. The assumed SOS of acrylic material is in the range of 2610–2750 m/s [5]. SOS measurements were performed eight times (twice a day for 4 days) in water; the water temperature was also recorded at the same time. The measured SOS was 2736 ± 1.3 m/s with a coefficient of variation (CV) of 0.05% (27.3 ± 0.6 °C). Extremely good reproducibility was obtained.

The specimen thickness dependency of SOS was also tested using 5-, 3-, and 2-mm-thick acrylic plates, which correspond to 5.5, 3.3, and 2.2

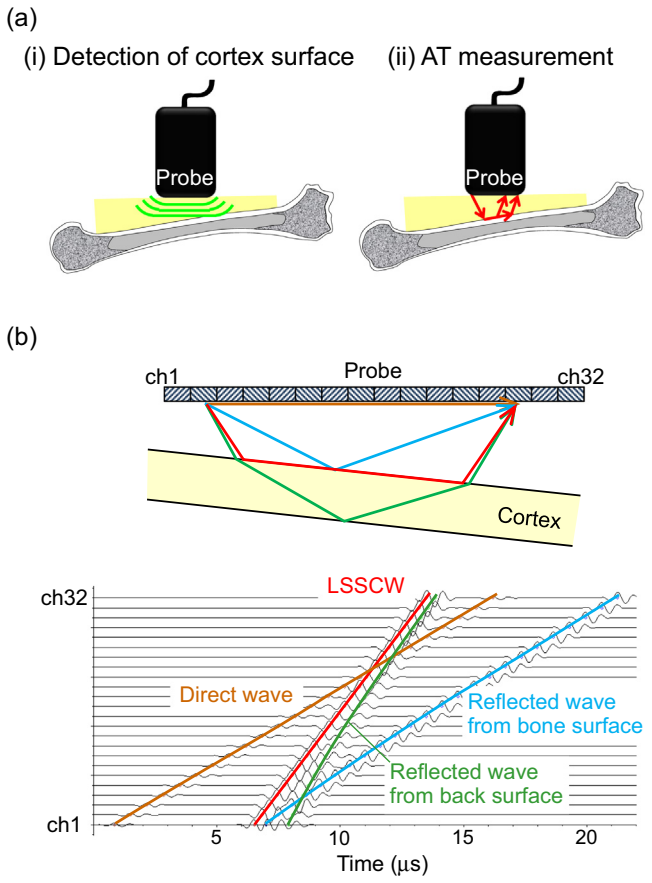

Fig. 2. Schematic representations of developed AT instrument features. (a) Two-step transmission/reception system including (i) cortex-surface monitoring phase (distribution of soft tissue thickness) and (ii) AT measurement phase, which was enabled by a probe with linearly arrayed multiple receivers. (b) Multiple receivers with 32 channels to separately detect necessary LSSCWs from other unnecessary signals inevitably generated when cortical bone is irradiated by ultrasonic waves.

times the wavelength, respectively. The measurements were performed approximately 200 times each in water with variations in the distance and angle between the probe and acrylic plate. This approach was adopted to simulate measurement of human legs with non-uniform soft tissue thickness. The measured SOSs for the 5-, 3-, and 2-mm-thick plates were 2733 ± 5 (CV 0.20%), 2727 ± 4 (CV 0.16%), and 2736 ± 13 m/s (CV 0.49%), respectively. For all measurements, an SOS of 2732 ± 5 m/s (CV 0.17%) was recorded, showing the good precision of our instrument.

2.5. Human cadaver bone specimens

2.5.1. Femur blocks for Study_1

Seventeen femurs of Japanese human cadavers (male: 10; female: 7) donated to Osaka City University Hospital were used with an approval by the Ethics Committee of Osaka City University Hospital. The cadavers were stored in 10% formalin neutral buffer solution. In each case, a rectangular cortical bone block with dimensions of approximately 10 mm × 10 mm in the axial and tangential directions was removed from medial part of the proximal left femur (Fig. 3). The cadaver age range was 70–94 years (83 ± 7 years). The periosteal and endosteal surfaces were minimally ground to obtain flat planes. All specimen surfaces were finished with #2000 silicon carbide paper. The measurements were performed in water at 26 °C.

2.5.2. Tibia with soft tissue for Study_2

Nine tibias of Japanese human cadavers (male: 6; female: 3) donated to Osaka University Hospital were used with an approval by the Ethics Committee of Osaka University Hospital. The cadavers were stored in 10% formalin neutral buffer solution. The age range of the cadavers was 81–98 years (86 ± 7 years). Axial cSOS measurement via the AT method was performed on the right tibial diaphysis. The midshaft corresponding to the center of the AT measurement was cross-sectioned at approximately 10-mm thickness; then, the axial specimen surfaces were finished with #2000 silicon carbide paper. cSOS measurements by the DT method were performed at the AT measurement location along the axial direction. All ultrasound measurements were performed in water at 26 °C. Finally, the correlation between the cSOSs measured by the AT and DT methods was analyzed to validate the device setup used in this study.

2.6. Measurement of volumetric BMD

The vBMD was measured at the center part of the cSOS measurement region using a peripheral quantitative computed tomography (XCT Research SA+, Stratec Medizintechnik GmbH, Birkenfeld, Germany) with a resolution of 240 × 240 × 460 μm^3. The data for each voxel were exported in ASCII format (CSV file) to Microsoft Excel software. Values exceeding a threshold value of 690 mg/cm^3 were judged to indicate cortical bone.

2.7. Analysis of apatite preferential orientation

To assess the degree of preferential orientation of the apatite *c*-axis, microbeam X-ray diffraction (μXRD) analysis was performed (M18XHF22-SR, Mac Science Co., Yokohama, Japan). Cu-Kα radiation generated at a tube voltage and tube current of 40 kV and 90 mA, respectively, was used. A metal collimator with a diameter of 50 or 100 μm was employed. The specimen was fixed, swung, and rotated through the appropriate range of Euler angles to obtain sufficient diffraction intensity. The detailed conditions for μXRD analysis are described in a previous study [15]. Briefly, the scattered diffraction was counted with a curved position-sensitive proportional X-ray counter for 1000 s to obtain an XRD profile. The two representative diffraction peaks for apatite, (002) and (310) appearing at Bragg angles (2θ) of 25.9° and 39.8°, respectively, were detected. The degree of preferential alignment of the apatite *c*-axis was determined as an intensity ratio of (002)/(310). Randomly oriented hydroxyapatite (NIST #2910: calcium hydroxyapatite) powder had an intensity ratio of 2 in this μXRD system; therefore, detected values > 2 indicated the presence of anisotropic apatite *c*-axis orientation in the analyzed direction [15]. The measurements were performed three times and the average values were used.

2.8. Statistical analyses

The quantitative results are expressed in mean ± standard deviation (SD) form. The statistical significance among the three means was determined using one-way analysis of variance (ANOVA) with post hoc multiple comparison analyses. For multiple comparison analyses, Tukey honestly significant difference (HSD) or Games-Howell comparisons were conducted on the basis of the homoscedasticity test, where appropriate. Pearson's correlations and multiple linear regression analyses were used to determine significant determinants for cSOS. In the multiple linear regression analysis, the vBMD and the degree of apatite orientation were considered independent variables. The multiple regression coefficient (β) was used to identify the dominant determinant. A *P*-value < 0.05 was considered statistically significant. SPSS version 14.0 J software (SPSS Japan Inc., Tokyo, Japan) for Microsoft Windows was used for all statistical analyses.

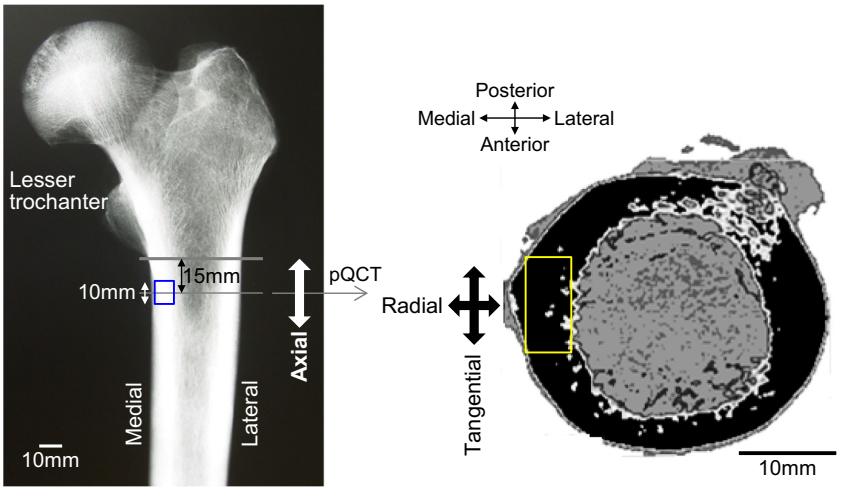

Fig. 3. Area from which rectangular cortical bone block was obtained.

3. Results

For all measured parameters, there were no significant differences between male and female. Therefore, the data are reported without separation of sex.

3.1. Study_1: correlation between tri-directional anisotropy of cSOS given by DT method and bone microstructure

3.1.1. Tri-directional anisotropy in cSOS and degree of apatite orientation in femoral cortex

In the DT measurement of the rectangularly shaped femoral cortical bone specimen, the axial cSOS (3870 ± 66 m/s) was the highest, followed by the tangential (3411 ± 94 m/s) and radial (3320 ± 85 m/s) cSOSs (Fig. 4(a)). The anisotropy ratios (the squared ultrasound velocities in two directions) were 1.29 (axial/tangential) and 1.36 (axial/radial). The degree of apatite orientation exhibited similar tendencies, being highest in the axial direction, followed by the tangential and radial directions (Fig. 4(b)). The degrees of apatite orientation in the tangential and radial directions were approximately 2, indicating the lack of a prominent preferential apatite orientation in these directions. Thus, the femoral cortical bone exhibits distinct preferential apatite orientation along the axial direction.

3.1.2. Correlations of cSOS vs vBMD, and SOS vs apatite orientation

The vBMD positively and independently correlated with the cSOSs in each direction (Fig. 5(a)). It is apparent that the data plots for the three directions shown in Fig. 5(a) do not overlap on a single line and that they each form a separate linear relationship; thus, different cSOSs were derived from a single vBMD. With regard to the correlation between the cSOS and vBMD, the strength (i.e., the largeness of the Pearson's correlation coefficient (r)) and significance (the P-value smallness) of the correlation were highest in the radial direction, followed by the tangential direction. Thus, the lowest values were in the axial direction. In contrast, the degree of preferential apatite orientation positively correlated with the cSOS in the axial direction only; no significant correlations were found in the tangential and radial directions (Fig. 5(b)). There was no significant multicollinearity between the vBMD and the degree of preferential apatite orientation in all directions ($r = 0.17$, $P > 0.05$; $r = 0.44$, $P > 0.05$; and $r = 0.11$, $P > 0.05$ in the axial, tangential, and radial directions, respectively). A multiple regression analysis was performed (Table 1). In each of the three directions, the multiple regression result was statistically significant, with the adjusted coefficients of determination (R^2) being approximately 0.7. On the basis of the relative magnitude of the multiple regression coefficients (β) and P-values for vBMD and apatite orientation, the apatite orientation was determined to be the stronger contributing factor to the cSOS in the axial direction. The vBMD contribution was larger in the tangential and radial directions. Overall, the apatite orientation was found to be a stronger determinant of the cSOS than vBMD, and the regression precision was remarkably high ($R^2 = 0.94$).

3.2. Study_2: cSOS measurement via AT method with 3-MHz ultrasound

3.2.1. Relation between cSOS values measured using DT and AT methods

The AT method was implemented on the medial surface of the tibia because of the minimal soft tissue. To assess the position dependency of the cSOS, which is important for precise diagnosis, measurements were

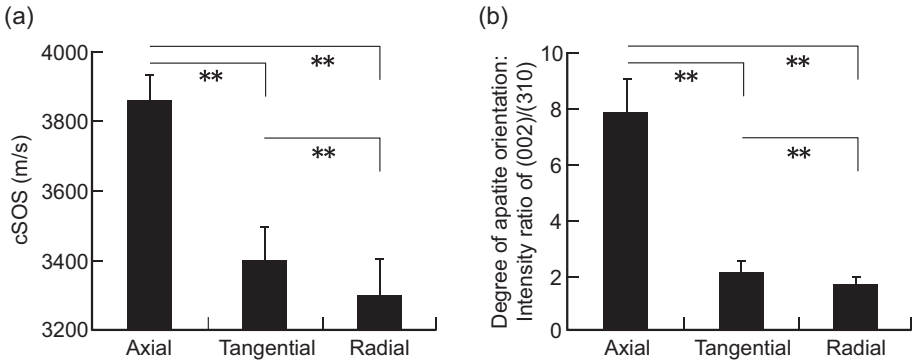

Fig. 4. Variations of (a) cSOS and (b) degree of apatite orientation in axial, tangential, and radial directions. **: $P < 0.01$.

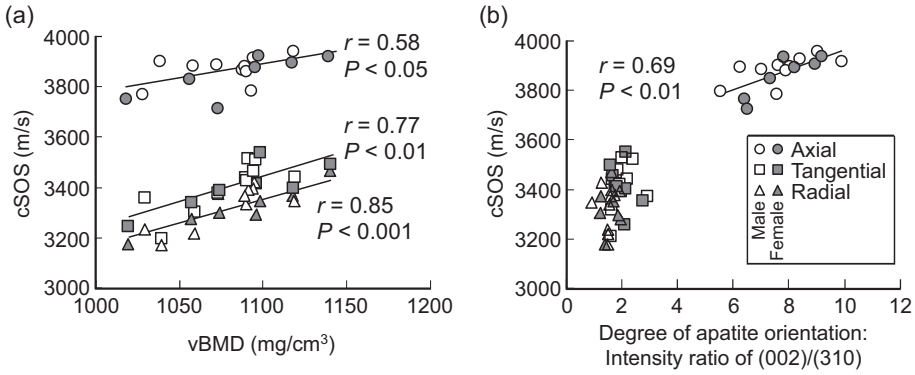

Fig. 5. Correlations between (a) cSOS and vBMD and (b) cSOS and degree of apatite orientation in axial, tangential, and radial directions. The straight lines represent significant correlations between the parameters.

Table 1
R^2, β, and P values derived from multiple regression analysis. NS: not significant.

	Result of multiple regression		Contribution analysis			
			vBMD		Apatite orientation	
	R^2	P	β	P	β	P
Axial	0.66	< 0.001	0.48	< 0.001	0.61	< 0.001
Tangential	0.72	< 0.001	0.96	< 0.001	0.44	< 0.05
Radial	0.72	< 0.001	0.87	< 0.001	0.15	NS
Overall	0.94	< 0.001	0.23	< 0.001	0.96	< 0.001

performed at three positions, i.e., the anterior, middle, and posterior, which were separated by 10, 15, and 20 mm from the anterior border, respectively (Fig. 6(a, b)). Fig. 6(c) shows the correlation between the cSOSs along the tibial axial direction measured using the DT and AT methods. A significant and positive correlation was identified; therefore, our instrument for implementation of the AT method is valid for cSOS determination despite the interposition of soft tissue.

3.2.2. cSOS variation depending on anteroposterior position

Fig. 7(a, b) shows the variation in the apatite orientation and cSOS with position. For both the apatite orientation and cSOS, the values decreased from anterior to posterior ($P < 0.05$ according to a one-way ANOVA). Note that the bone-material microstructure and properties exhibited considerable position dependency. The QUS measurement sensitively detected these characteristics. Standardization of the position to be measured is required in clinical settings.

3.2.3. Correlations of cSOS vs vBMD, and cSOS vs apatite orientation

Fig. 8 shows the correlation between the (a) cSOSs and vBMD and (b) cSOSs and apatite orientation. The apatite orientation was positively correlated with the cSOS. According to the multiple regression analysis, the β and P values for apatite orientation were 0.82 and $< 1 \times 10^{-6}$, respectively. These results indicate that the degree of apatite orientation was a dominant contributory factor to the cSOS in this case.

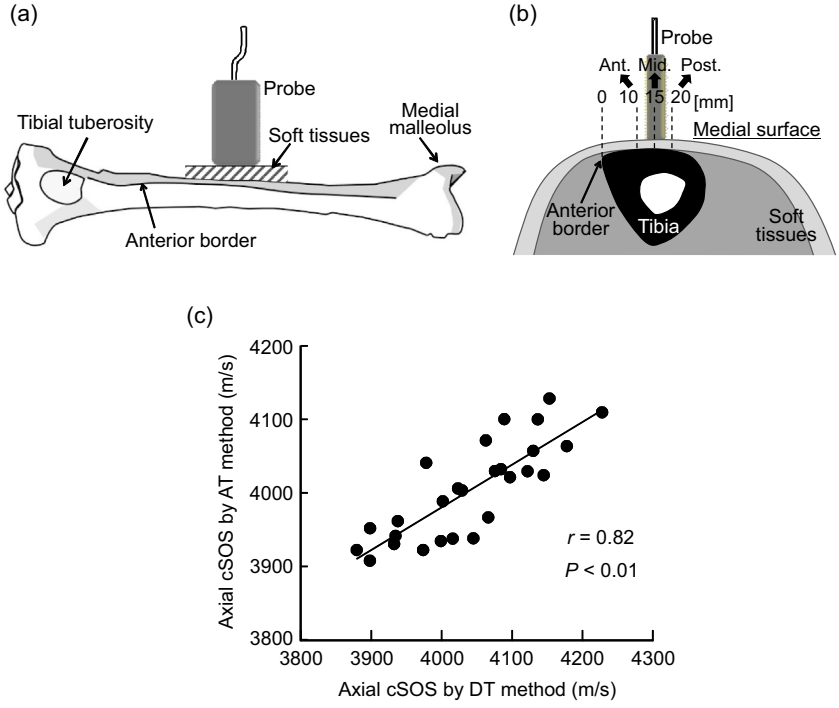

Fig. 6. (a) Schematic representation of measurement of tibial cSOS via AT method. (b) Representation of measurement positions (anterior, middle, and posterior) on tibial medial surface. (c) Correlation between cSOS values measured using AT and DT methods.

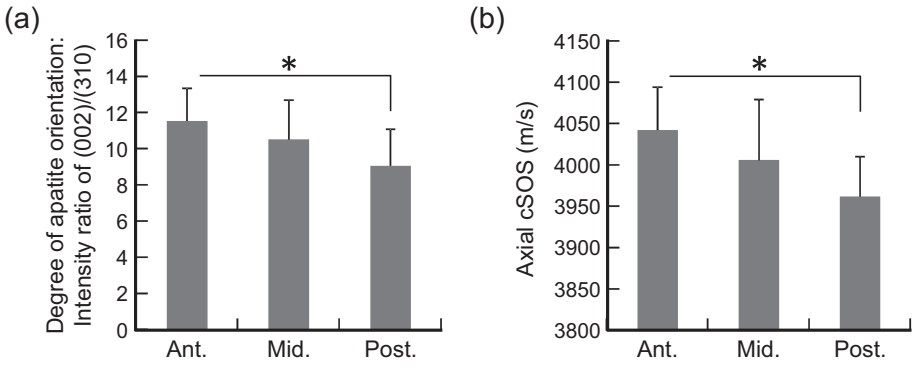

Fig. 7. (a) Variation of degree of apatite orientation in axial direction and (b) variation of axial cSOS depending on measurement position. *: $P < 0.01$.

4. Discussion

We developed a novel instrument to measure cortical SOS via the AT method. Our instrument is characterized by (i) its cortical bone surface-morphology detection system, which works to correct the ultrasound transmission distance, and (ii) use of relatively high-frequency ultrasound (3 MHz) that enables thickness-independent cSOS measurement, even for a thin cortex. Because of the bone surface-morphology detection/correction system, our instrument can be applied to several bone types such as the tibia, ulna, radius, and mandible, which are covered by relatively thin soft tissue. Moreover, our instrument is expected to be beneficial for screening of osteoporotic alterations of bone material, because the cortex of osteoporotic bone is generally thin. The cSOS measured by the AT method in this study was found to be highly correlated with that measured by the well-accepted conventional DT method, indicating the validity of our instrument for AT measurement. A slight difference was noted between the two cSOS values (i.e., the slope of the approximate line in Fig. 6 is not equal to 1). In the AT method, the cSOS tends to be most strongly influenced by the outer cortical bone [6]; therefore, variation of the bone microstructure along with the cortical thickness is possibly related to the cSOS difference between the two methods.

In this study, using either the DT or AT method, it was revealed that QUS strongly reflects the anisotropic microstructure of human long bones. Tri-directional anisotropy in the cSOS for human bone was revealed for the first time (Study_1). The findings are similar to those previously reported for bovine femurs [23]. In the human femur, the axial cSOS was found to be highest, followed by the tangential and radial cSOSs. This cSOS order is in good agreement with the degree of apatite orientation. In the tangential and radial directions, the vBMD exhibited correlation with the cSOS (Fig. 5a). This is because no prominent preference in apatite orientation was observed along these directions, as represented by the constant value of the μXRD intensity ratio of approximately 2 (Fig. 4b). In contrast, the cSOS in the axial direction correlated with either the degree of apatite orientation (Fig. 5b) or vBMD (Fig. 5a); the contribution was higher for the apatite orientation according to multiple regression analysis (Table 1). These statistical analyses demonstrate that the tangential and radial cSOS indicate the vBMD, whereas the axial cSOS more strongly reflects the degree of apatite orientation along the axial bone axis. In this study, tangential cSOS was determined by the DT method using blocked bone specimens, which cannot be applied in clinical settings. The development of a small probe that fits the transverse width of bones allows noninvasive measurement of both axial and tangential cSOSs, which strongly reflect apatite orientation and vBMD, respectively.

With regard to biomechanics, the axial direction is mechanically important for long bones because the *in vivo* mechanical stress is principally applied in this direction [24]. It is well known that long bones are mechanically strengthened in the axial direction [25,26]; this is at least in part due to preferential orientation of both apatite and collagen in this direction [15,27]. Moreover, in some pathological long bones, the apatite orientation in the axial direction changes significantly. For example, in long bones affected by osteopetrosis [28], cancer metastasis [29,30], weightlessness by sciatic neurectomy [31], and stress shielding due to use of high-modulus metallic implants [32], remarkable deterioration of the apatite orientation and Young's modulus in the axial direction have been observed. This deterioration of material properties in the tangential and radial directions is not necessarily detectable, because the apatite orientation in the tangential and radial directions is inevitably close to random. Therefore, assessment of axial properties is more effective for evaluation of the mechanical integrity of the long-bone cortex and screen bone disorders.

Anisotropy in the long-bone cortex has been revealed to have an impact on cSOS measurement as a function of cortical thickness [21].

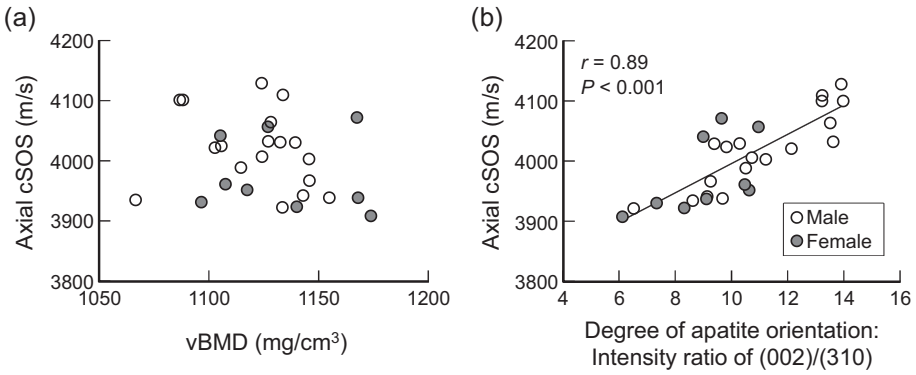

Fig. 8. Correlations between (a) axial cSOS and vBMD and (b) axial cSOS and degree of apatite orientation in axial direction. The straight line represents significant correlations between the parameters.

The cortical thickness is a very important factor in AT measurement because the cSOS decreases independently of the material property when the thickness is below a certain threshold (i.e., the threshold thickness) [14,21]. To assess the intrinsic material properties, the cortex must be adequately thick. According to numerical simulations based on a three-dimensional finite difference method, anisotropy in bone reduces the threshold thickness by half in comparison to that obtained when the bone is assumed to be isotropic. In anisotropic bone, the thickness dependence of the cSOS arises for a cortex thinner than half the wavelength; however, when isotropic bone is assumed, this dependence appears for any cortex thinner than the wavelength [21]. For the present study involving 3-MHz ultrasound with 1.33-mm wavelength (when the cSOS is approx. 4000 m/s), in theory, a cortex thicker than approx. 0.7 mm can be properly measured. In this work, the tibial cortical thicknesses at the measurement points were in the range of approx. 1.7–4.6 mm; therefore, the obtained cSOS data should appropriately reflect the bone material properties. In general, as the typical cortical thickness is reported to range between 1 and 7 mm [21], ultrasound procedures with higher frequencies than approx. 3 MHz are highly recommended. Use of 1-MHz ultrasound (for which the threshold thickness should be 2 mm) can potentially generate guide waves, with cSOS values reduced by the thickness effect possibly being obtained from a portion of the subjects.

In this study, we used the human tibia and femur, allowing comparison of the material properties of these two bones. The tibia and femur specimens were derived from different donors, but the age distributions were similar (83 ± 7 years for tibia donors and 86 ± 7 years for femur donors, $P > 0.05$). Either the axial cSOS measured by the DT setup or the degree of apatite orientation in the axial direction was significantly higher for the tibia. The axial cSOS and degree of apatite orientation for the femur and tibia were 3870 ± 66 m/s and 4042 ± 77 m/s ($P < 0.001$), and 7.74 ± 1.16 and 10.35 ± 1.74 ($P < 0.001$), respectively. According to the literature, the anisotropy ratio in the Young's modulus (calculated as the ratio of the axial modulus to the vertical modulus) is in the range of 1.35–1.58 for the human tibia [25,26,33] and of 1.16–1.41 for the femur [34,35]; the tibia exhibits higher anisotropy with regard to the axial direction. Our findings agree well with these reports. Thus, the criteria for screening bone disorders should be individually determined for each bone type.

The human bone specimens employed in this study were preserved with formalin to prevent degradation and infection. Because rectangular specimens were required, living subjects could not be used. However, it is difficult to acquire a sufficient number of fresh or frozen cadavers in Japan. Further, the potential influence of the formalin fixation on the cSOS measurements cannot be excluded, which is a limitation of this study. The effect of fixation on sound velocity in the cortex has been noted for absolute values only [36], and not for relative magnitudes, including correlations [37]. Analyses of fresh-frozen bones or patients' bones are expected to be able to detect not only the apatite orientation but also compositional changes in the bone [38] that might relate to aging and diseases, which would expand the applicability of this method. Since its methodological validity has been guaranteed, it would be desirable to apply our instrument to fresh-frozen or patients' bones in future research.

To test the potential of our instrument for screening osteoporotic bone degradation, future studies must clarify the osteoporotic changes in the cSOS on the basis of its relationship with the changes in the bone material properties, not only via vBMD but also via apatite orientation (bone quality parameter based on the material anisotropy). It is possible that osteoporotic bone exhibits changes in the material anisotropy independent of the vBMD. One such example is the reported increase in the preferential apatite orientation along the craniocaudal direction in an ovariectomized rat vertebral cortex, despite decreasing vBMD [39–41]. Ultrasonic and material investigation of both cadavers and living patients with osteoporosis should be targeted as the next research challenge. Moreover, as QUS is limited to peripheral bone sites only, the correlations between QUS results and the fracture risk of bone sites in which fractures frequently occur, such as the femoral neck, proximal femur, and vertebrae, should be established.

5. Conclusions

We developed a QUS-AT instrument with a cortical bone surface-morphology detection/correction system and ultrasound with a relatively high frequency of 3 MHz. The cSOS was demonstrated to strongly reflect the anisotropy in the bone material, which is characterized by preferential orientation of the apatite *c*-axis as a bone quality parameter. The developed AT instrument yielded comparable results to those obtained using the well-established DT method, indicating the validity of our methodology for evaluating the material integrity of the human long-bone cortex.

Declaration of Competing Interest

Takuya Ishimoto, Ryoichi Suetoshi, Dorian Cretin, Koji Hagihara, Jun Hashimoto, Akio Kobayashi, and Takayoshi Nakano declare that they have no conflicts of interest.

Acknowledgments

This work was partly supported by Grants-in-Aid for Scientific Research from the Japan Society for the Promotion of Science (JSPS) [grant numbers JP18H05254 and JP19H00827].

Authors' roles

Conceptualization: TN and RS. Methodology: TI, RS, DC, KH, JH, AK, and TN. Investigation: TI, RS, and DC. Formal analysis: TI, RS, and TN. Writing - original draft: TI, RS, and KH. Writing - review and editing: TI, RS, DC, KH, and TN. All authors approved the final version of the manuscript. TN takes responsibility for the integrity of the data analysis.

References

[1] K. Thomsen, D.B. Jepsen, L. Matzen, A.P. Hermann, T. Masud, J. Ryg, Is calcaneal quantitative ultrasound useful as a prescreen stratification tool for osteoporosis? Osteoporos. Int. 26 (2015) 1459–1475, https://doi.org/10.1007/s00198-014-3012-y.

[2] S. Rouillard, N.E. Lane, Hepatic osteodystrophy, Hepatology 33 (2001) 301–307, https://doi.org/10.1053/jhep.2001.20533.

[3] G. Holzer, G. von Skrbensky, L.A. Holzer, W. Pichl, Hip fractures and the contribution of cortical versus trabecular bone to femoral neck strength, J. Bone Miner. Res. 24 (2009) 468–474, https://doi.org/10.1359/jbmr.081108.

[4] T. Tang, P.A. Cripton, P. Guy, H.A. McKay, R. Wang, Clinical hip fracture is accompanied by compression induced failure in the superior cortex of the femoral neck, Bone 108 (2018) 121–131, https://doi.org/10.1016/j.bone.2017.12.020.

[5] M. Daugschies, K. Rohde, C.-C. Glüer, R. Barkmann, The preliminary evaluation of a 1 MHz ultrasound probe for measuring the elastic anisotropy of human cortical bone, Ultrasonics 54 (2014) 4–10, https://doi.org/10.1016/j.ultras.2013.07.004.

[6] S. Prevrhal, T. Fuerst, B. Fan, C. Njeh, D. Hans, M. Uffmann, S. Srivastav, H.K. Genant, Quantitative ultrasound of the tibia depends on both cortical density and thickness, Osteoporos. Int. 12 (2001) 28–34, https://doi.org/10.1007/s001980170154.

[7] A.J. Foldes, A. Rimon, D. Keinan, M. Popovtzer, Quantitative ultrasound of the tibia: a novel approach for assessment of bone status, Bone 17 (1995) 363–367, https://doi.org/10.1016/S8756-3282(95)00244-8.

[8] D. Hans, S.K. Srivastav, C. Singal, R. Barkmann, C.F. Njeh, E. Kantorovich, C.C. Glüer, H.K. Genant, Does combining the results from multiple bone sites measured by a new quantitative ultrasound device improve discrimination of hip fracture? J. Bone Miner. Res. 14 (1999) 644–651, https://doi.org/10.1359/jbmr.1999.14.4.644.

[9] M. Muller, P. Moilanen, E. Bossy, P. Nicholson, V. Kilappa, J. Timonen, M. Talmant, S. Cheng, P. Laugier, Comparison of three ultrasonic axial transmission methods for bone assessment, Ultrasound Med. Biol. 31 (2005) 633–642, https://doi.org/10.1016/j.ultrasmedbio.2005.02.001.

[10] V. Egorov, A. Tatarinov, N. Sarvazyan, R. Wood, L. Magidenko, S. Amin, S. Khosla, R.J. Ruh, J.M. Ruh, A. Sarvazyan, Osteoporosis detection in postmenopausal

women using axial transmission multi-frequency bone ultrasonometer: clinical findings, Ultrasonics 54 (2014) 1170–1177, https://doi.org/10.1016/j.ultras.2013.08.017.
[11] P. Moilanen, V. Kilapp, P.H.F. Nicholson, J. Timonen, S. Cheng, Thickness sensitivity of ultrasound velocity in long bone phantoms, Ultrasound Med. Biol. 30 (2004) 1517–1521, https://doi.org/10.1016/j.ultrasmedbio.2004.08.017.
[12] J. Foiret, J.G. Minonzio, C. Chappard, M. Talmant, P. Laugier, Combined estimation of thickness and velocities using ultrasound guided waves: a pioneering study on in vitro cortical bone samples, IEEE Trans. Ultrason. Ferroelectr. Freq. Control 61 (2014) 1478–1488, https://doi.org/10.1109/TUFFC.2014.3062.
[13] Q. Vallet, N. Bochud, C. Chappard, P. Laugier, J.G. Minonzio, In vivo characterization of cortical bone using guided waves measured by axial transmission, IEEE Trans. Ultrason. Ferroelectr. Freq. Control 63 (2016) 1361–1371, https://doi.org/10.1109/TUFFC.2016.2587079.
[14] J.G. Minonzio, N. Bochud, Q. Vallet, Y. Bala, D. Ramiandrisoa, H. Follet, D. Mitton, P. Laugiera, Bone cortical thickness and porosity assessment using ultrasound guided waves: an ex vivo validation study, Bone 116 (2018) 111–119, https://doi.org/10.1016/j.bone.2018.07.018.
[15] T. Nakano, K. Kaibara, Y. Tabata, N. Nagata, S. Enomoto, E. Marukawa, Y. Umakoshi, Unique alignment and texture of biological apatite crystallites in typical calcified tissues analyzed by microbeam X-ray diffractometer system, Bone 31 (2002) 479–487, https://doi.org/10.1016/S8756-3282(02)00850-5.
[16] A. Tatarinov, V. Egorov, N. Sarvazyan, A. Sarvazyan, Multi-frequency axial transmission bone ultrasonometer, Ultrasonics 54 (2014) 1162–1169, https://doi.org/10.1016/j.ultras.2013.09.025.
[17] T. Ishimoto, T. Nakano, Y. Umakoshi, M. Yamamoto, Y. Tabata, Degree of biological apatite c-axis orientation rather than bone mineral density controls mechanical function in bone regenerated using recombinant bone morphogenetic protein-2, J. Bone Miner. Res. 28 (2013) 1170–1179, https://doi.org/10.1002/jbmr.1825.
[18] T. Shinno, T. Ishimoto, M. Saito, R. Uemura, M. Arino, K. Marumo, T. Nakano, M. Hayashi, Comprehensive analyses of how tubule occlusion and advanced glycation end-products diminish strength of aged dentin, Sci. Rep. 6 (2016) srep19849, , https://doi.org/10.1038/srep19849.
[19] B. Viswanath, R. Raghavan, U. Ramamurty, N. Ravishankar, Mechanical properties and anisotropy in hydroxyapatite single crystals, Scr. Mater. 57 (2007) 361–364, https://doi.org/10.1016/j.scriptamat.2007.04.027.
[20] C.F. Njeh, C.M. Boivin, C.M. Langton, The role of ultrasound in the assessment of osteoporosis: a review, Osteoporos. Int. 7 (1997) 7–22, https://doi.org/10.1007/BF01623454.
[21] E. Bossy, M. Talmant, P. Laugier, Three-dimensional simulations of ultrasonic axial transmission velocity measurement on cortical bone models, J. Acoust. Soc. Am. 115 (2004) 2314–2324, https://doi.org/10.1121/1.1689960.
[22] H. Asai, H. Kanai, Noninvasive measurement of stiffness and density of bone for its diagnosis using ultrasound, J. Med. Ultrason. 29 (2002) 129–135, https://doi.org/10.1007/BF02481235.
[23] Y. Yamato, M. Matsukawa, T. Yanagitani, K. Yamazaki, H. Mizukawa, A. Nagano, Correlation between hydroxyapatite crystallite orientation and ultrasonic wave velocities in bovine cortical bone, Calcif. Tissue Int. 82 (2008) 162–169, https://doi.org/10.1007/s00223-008-9103-z.
[24] T. Wehner, U. Wolfram, T. Henzler, F. Niemeyer, L. Claes, U. Simon, Internal forces and moments in the femur of the rat during gait, J. Biomech. 43 (2010) 2473–2479, https://doi.org/10.1016/j.jbiomech.2010.05.028.
[25] J.G. Swadener, J.Y. Rho, G.M. Pharr, Effects of anisotropy on elastic moduli measured by nanoindentation in human tibial cortical bone, J. Biomed. Mater. Res. 57 (2001) 108–112, https://doi.org/10.1002/1097-4636(200110)57:1<108::AID-JBM1148>3.0.CO;2-6.
[26] J.Y. Rho, M.E. Roy, T.Y. Tsui, G.M. Phar, Elastic properties of microstructural components of human bone tissue as measured by nanoindentation, J. Biomed. Mater. Res. 45 (1999) 48–54, https://doi.org/10.1002/(SICI)1097-4636(199904)45:1<48::AID-JBM7>3.0.CO;2-5.
[27] R.B. Martin, J. Ishida, The relative effects of collagen fiber orientation, porosity, density, and mineralization on bone strength, J. Biomech. 22 (1989) 419–426, https://doi.org/10.1016/0021-9290(89)90202-9.
[28] T. Ishimoto, B. Sato, J.-W. Lee, T. Nakano, Co-deteriorations of anisotropic extracellular matrix arrangement and intrinsic mechanical property in c-src deficient osteopetrotic mouse femur, Bone 103 (2017) 216–223, https://doi.org/10.1016/j.bone.2017.06.023.
[29] A. Sekita, A. Matsugaki, T. Nakano, Disruption of collagen/apatite alignment impairs bone mechanical function in osteoblastic metastasis induced by prostate cancer, Bone 97 (2017) 83–93, https://doi.org/10.1016/j.bone.2017.01.004.
[30] A. Sekita, A. Matsugaki, T. Ishimoto, T. Nakano, Synchronous disruption of anisotropic arrangement of the osteocyte network and collagen/apatite in melanoma bone metastasis, J. Struct. Biol. 197 (2016) 260–270, https://doi.org/10.1016/j.jsb.2016.12.003.
[31] J. Wang, T. Ishimoto, T. Nakano, Unloading-induced degradation of the anisotropic arrangement of collagen/apatite in rat femurs, Calcif. Tissue Int. 100 (2017) 87–97, https://doi.org/10.1007/s00223-016-0200-0.
[32] Y. Noyama, T. Miura, T. Ishimoto, T. Itaya, M. Niinomi, T. Nakano, Bone loss and reduced bone quality of the human femur after total hip arthroplasty under stress-shielding effects by titanium-based implant, Mater. Trans. 53 (2012) 565–570, https://doi.org/10.2320/matertrans.M2011358.
[33] Z. Fan, J.G. Swadener, J.Y. Rho, M.E. Roy, G.M. Pharr, Anisotropic properties of human tibial cortical bone as measured by nanoindentation, J. Orthop. Res. 20 (2002) 806–810, https://doi.org/10.1016/S0736-0266(01)00186-3.
[34] T. Hofmann, F. Heyroth, H. Meinhard, W. Franzel, K. Raum, Assessment of composition and anisotropic elastic properties of secondary osteon lamellae, J. Biomech. 39 (2006) 2282–2294, https://doi.org/10.1016/j.jbiomech.2005.07.009.
[35] G. Franzoso, P.K. Zysset, Elastic anisotropy of human cortical bone secondary osteons measured by nanoindentation, J. Biomech. Eng. 131 (2009) 021001, , https://doi.org/10.1115/1.3005162.
[36] E.-M. Lochmüller, F. Eckstein, J.B. Zeller, R. Steldinger, R. Putz, Comparison of quantitative ultrasound in the human calcaneus with mechanical failure loads of the hip and spine, Ultrasound Obstet. Gynecol. 14 (1999) 125–133, https://doi.org/10.1046/j.1469-0705.1999.14020125.x.
[37] C.C. Glüer, R.K. Barkmann, Quantitative ultrasound: use in the detection of fractures and in the assessment of bone composition, Curr. Osteoporos. Rep. 1 (2013) 98–104, https://doi.org/10.1007/s11914-996-0003-8.
[38] G. Pöpperl, E.M. Lochmüller, H.J. Becker, G. Mall, M. Steinlechner, F. Eckstein, C.C. Glüer, R.K. Barkmann, Determination of calcaneal ultrasound properties ex situ: reproducibility, effects of storage, formalin fixation, maceration, and changes in anatomic measurement site, Calcif. Tissue Int. 65 (1999) 192–197, https://doi.org/10.1007/s002239900681.
[39] M. Tanaka, A. Matsugaki, T. Ishimoto, T. Nakano, Evaluation of crystallographic orientation of biological apatite at vertebral cortical bone in ovariectomized cynomolgus monkey treated with minodronic acid and alendronate, J. Bone Miner. Metab. 34 (2016) 234–241, https://doi.org/10.1007/s00774-015-0658-2.
[40] A. Shiraishi, S. Miyabe, T. Nakano, Y. Umakoshi, M. Ito, M. Mihara, The combination therapy with alfacalcidol and risedronate improves the mechanical property in lumbar spine by affecting the material properties in an ovariectomized rat model of osteoporosis, BMC Musculoskelet. Disord. 10 (2009), https://doi.org/10.1186/1471-2474-10-66 paper #66.
[41] R. Ozasa, T. Ishimoto, S. Miyabe, J. Hashimoto, M. Hirao, H. Yoshikawa, T. Nakano, Osteoporosis changes collagen/apatite orientation and Young's modulus in vertebral cortical bone of rat, Calcif. Tissue Int. 104 (2019) 449–460, https://doi.org/10.1007/s00223-018-0508-z.